Steel and Composite Structures, Vol. 1, No. 3 (2001) 269-282
DOI: http://dx.doi.org/10.12989/scs.2001.1.3.269

Cyclic behaviour of beam-to-column welded connections

Elena Mele†

Dipartimento di Analisi e Progettazione Strutturale (DAPS), Università di Napoli "Federico II", P.le Tecchio 80, 80125 Napoli, Italy

Luis Calado‡

Departamento de Engenharia Civil (DECivil), Instituto Superior Tecnico, Av. Rovisco Pais, 1049-001 Lisboa, Portugal

Antonello De Luca‡†

Dipartimento di Analisi e Progettazione Strutturale (DAPS), Università di Napoli "Federico II", P.le Tecchio 80, 80125 Napoli, Italy

Abstract. In this paper the results of an experimental program devoted to the assessment of the cyclic behaviour of full scale, European type, beam-column subassemblages with welded connections are presented. Six tests (five cyclic and one monotonic) have been carried out on three different series of specimens, encompassing a total of eighteen tests. The three specimen series have been designed with the aim of defining the effect of the column size on the connection behaviour, under different applied loading histories. The tests have evidenced the effect of the column size and panel zone design and of the applied loading history on the cyclic behaviour and failure modes of the connections.

Key words: welded connections; cyclic tests; loading histories; rotation capacity; panel zone; failure modes.

1. Introduction

The confidence of structural engineering in welded moment resisting frames (WMRFs) was strongly compromised by the performances observed in the earthquakes of Northridge (1994) and Hyogoken-Nanbu (1995). Following these earthquakes, extensive unexpected brittle connection damage were detected in several frames, thus discovering the alarming problem of the high seismic vulnerability of the welded steel framed structures. The brittle modes of failure occurred at the beam-to-column joints have been defined "*unexpected*", since the WMRF connections were usually considered as the ones characterised by the more stable and ductile behaviour, giving rise

†Assistant Professor
‡Associate Professor
‡†Professor

to large rotational capacity and energy dissipation. It should be underlined though that, as reported by (Bertero *et al*. 1994), almost all the types of failures occurred as a result of the Northridge seismic shaking, had been observed in past experimental tests carried out in U.S.A., as well as in Japan and Europe. However the experimental behaviour of the welded connections appears highly and perhaps randomly variable.

Starting from these observations, significant research efforts have been undertaken in the United States (Mahin *et al*. 1996, Malley 1998), in Japan (Tanaka *et al*. 1997, Nakashima *et al*. 1998) and also in Europe (Mele *et al*. 1997, Plumier *et al*. 1998, Taucer *et al*. 1998, Calado *et al*. 1999, Calado and Mele 2000), in order to enrich the experimental data base and to assess the major parameters affecting the cyclic behaviour of beam-to-column connections.

In this context, a wide experimental program has been carried out at the Material and Structures Test Laboratory of the Instituto Superior Técnico of Lisbon on different types (both welded and bolted) of beam-to-column connections. The experimental tests have been performed on specimens representative of frame structure beam-to-column joints close to the ones typical of European design practice (beams less deep than the ones adopted in the current US design of SMRFs), with the aim of defining the effect of the column size and of the panel zone design on the connection behaviour, under different applied loading histories. Some preliminary experimental results on the welded connections have been presented in (Mele *et al*. 1997, Calado *et al*. 1999). In this paper a complete overview on the experimental program carried out on welded connections is reported. In particular the experimental results are presented through hysteresis loops obtained in the increasing amplitude tests; further, the failure modes of the specimens under different loading histories are described, and the major factors affecting the cyclic behaviour, the failure mode and the rotation capacity are assessed.

2. The experimental program

2.1. Specimen geometry

A total of 18 beam-to-column fully welded joints (3 series ×6 specimens) have been designed, fabricated and tested up to failure under different loading histories. The specimens are T-shaped

Table 1 Beam and column section properties

	Beam Section	Column Section		
	All specimens	BCC5	BCC6	BCC8
	IPE 300	HE160B	HE200B	HE240B
Height (mm)	300	160	200	240
Width (mm)	150	160	200	240
t_w (mm)	7.1	8	9	10
t_f (mm)	10.7	13	15	17
I (mm^4)	83560×10^3	24920×10^3	56960×10^3	112600×10^3
W_{el} (mm^3)	557×10^3	311×10^3	570×10^3	938×10^3
W_{pl} (mm^3)	628×10^3	354×10^3	643×10^3	1053×10^3

beam-column subassemblages, consisting of a 1000 mm long beam and a 1800 mm long column. In the three types of specimens, respectively appointed as BCC5, BCC6 and BCC8, the beam cross section is the same (IPE300), while the column cross section is varied, being respectively HE160B for the BCC5 series, HE200B for the BCC6 series, and HE240B for the BCC8 series. The main geometrical data of the beam and column sections adopted in the three specimen types (height, width, web thickness t_w, flange thickness t_f, moment of inertia I, elastic modulus W_{el}, plastic modulus W_{pl}) are reported in Table 1.

Due to the relative cross-section dimensions of column and beam in the three series of connection specimens, the beam plastic modulus is respectively larger, approximately equal and smaller than the column plastic modulus for the BCC5, BCC6 and BCC8 series.

In all specimens, the beam flanges have been connected to the column flange by means of complete joint penetration (CJP) groove welds, while fillet welds have been applied between both sides of the beam web and the column flange. The beam flange welds are double bevel complete joint penetration (CJP) butt welds, with no backing bars. Manual Metal Arc (MMA) welding procedure has been used with electrodes AWS 5.1 E 7018-1. Welding for the beam top and bottom flanges are both performed in the flat position, thus the root of the CJP welds is located on the interior side of both the top and the bottom flange. The continuity of the connection through the column has been ensured by 12 mm thick plate stiffeners, fillet welded to the column web and flanges.

2.2. Material properties

The structural steel used for the columns, beams, and stiffener plates is grade 235 Mpa, designated according to European international standard (CEN 1992) as S235 JR. Minimum values of the main material properties are: yield stress f_y = 235 Mpa; ultimate stress f_u = 360 MPa; elongation: 15%; Charpy V-notch energy: 27 Joules.

The basic monotonic stress-strain curve and the mechanical properties of the specimen steel components have been determined through coupon tension tests. The average values of the mechanical properties (yield stress, f_y, ultimate stress, f_u, and yield ratio, YR) for the beam and column flanges and web are provided in Table 2. In the same table are also provided the plastic and ultimate flexural capacities ($M_p=W_{pl}\times f_y$, $M_u=W_{pl}\times f_u$) of the beam and of the column, computed on the basis of the plastic section modulus W_{pl} and of the corresponding values of yield stress (f_y) and ultimate stress (f_u) of the section flanges obtained from the tension tests.

Table 2 Average values of material properties and derived flexural capacities

	BCC5				BCC6				BCC8			
	Beam		Column		Beam		Column		Beam		Column	
	IPE300		HE160B		IPE300		HE200B		IPE300		HE240B	
	flange	web	flange	web	flange	web	flange	web	flange	web	flange	web
f_y (MPa)	274.8	305.5	323.1	395.6	278.6	304.9	312.6	401.6	292	300	300	309
f_u (MPa)	404.6	412.6	460.2	490.1	398.8	411.4	434.9	489.8	445	450	457	469
YR	1.47	1.35	1.42	1.24	1.43	1.35	1.39	1.22	1.53	1.50	1.52	1.52
M_p (kNm)	166		118		169		198		183		316	
M_u (kNm)	234		157		242		276		280		482	

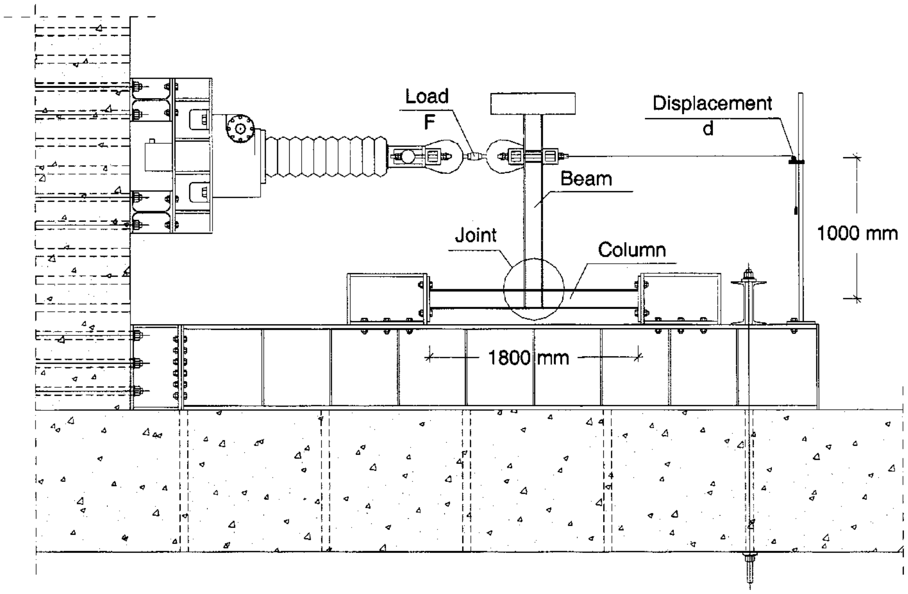

Fig. 1 Experimental set-up

2.3. Experimental set-up, instrumentation plan and loading histories

The test set-up, represented in Fig. 1, mainly consists in a foundation, a supporting girder, a reaction r.c. wall, a power jackscrew and a lateral frame. The power jackscrew (capacity 1000 kN, stroke ± 200 mm) is attached to a specific frame, pre-stressed against the reaction wall and designed to accommodate the screw backward movement. The specimen is connected to the supporting girder through two steel elements. The supporting girder is fastened to the reaction wall and to the foundation by means of pre-stressed bars.

An automatic testing technique was developed to allow computerised control of the power

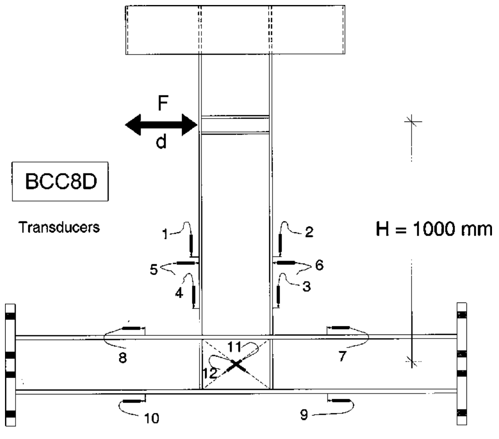

Fig. 2 Specimen instrumentation

Table 3 Loading histories

	BCC5			BCC6			BCC8		
	d [mm]	d/d_y	*d/H* [%]	*d* [mm]	d/d_y	*d/H* [%]	*d* [mm]	d/d_y	*d/H* [%]
A	C. type ± 50	C. type ± 5	C. type ± 5	C. type ± 50	C. type ± 5	C. type ± 5	C. type ± 50	C. type ± 5	C. type ± 5
B	C. type ± 75	C. type ± 7.5	C. type ± 7.5	C. type ± 75	C. type ± 7.5	C. type ± 7.5	C. type ± 37.5	C. type ± 3.75	C. type ± 3.75
BB	C. type ± 75	C. type ± 7.5	C. type ± 7.5	C. type ± 75	C. type ± 7.5	C. type ± 7.5			
C		S.I. type (ECCS)			S.I. type (ECCS)		C. type ± 75	C. type ± 7.5	C. type ± 7.5
D	C. type ± 37.5	C. type ± 3.75	C. type ± 3.75	C. type ± 37.5	C. type ± 3.75	C. type ± 3.75		S.I. type (ECCS)	
E		M. type			M. type		C. type ± 37.5	C. type ± 3.75	C. type ± 3.75
mon								M. type	

Legend: C. type = cyclic Constant amplitude loading history
S.I. type = cyclic Stepwise Increasing amplitude loading history
M. type = Monotonic loading history

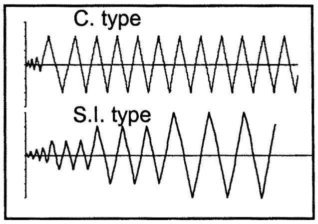

jackscrew, of the displacement and of all the transducers used to monitor the specimens during the testing process. Specimens have been instrumented with electrical displacement transducers (LVDTs), for carefully recording the various phenomena occurring during the tests. The same arrangement of LVDTs has been adopted for the three specimen types. The typical instrumentation set-up is provided in Fig. 2.

Each specimen type has been tested up to failure under several cyclic rotation histories. In particular

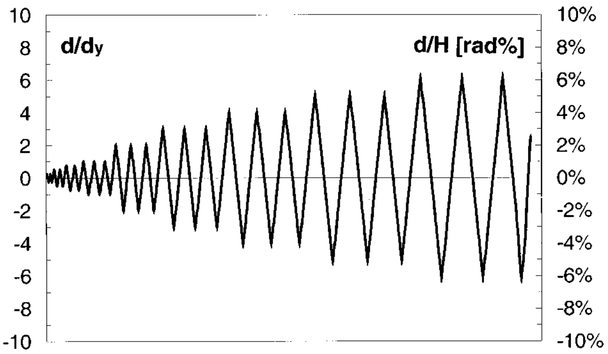

Fig. 3 ECCS cyclic stepwise increasing amplitude loading history

both constant-amplitude and stepwise-increasing-amplitude loading histories have been applied to the specimens. The complete set of loading histories is provided in Table 3, where each history is defined in terms of: cyclic amplitude of the applied beam tip displacement (d); cyclic amplitude of the applied beam tip displacement normalised to theoretical value of the specimen yield displacement d_y (d/d_y); cyclic amplitude of the applied interstory drift angle (d/H), i.e., d normalised to the distance between the beam tip and the column centreline H.

The stepwise increasing amplitude tests have been carried out according to the basic loading history recommended in (ECCS 1986), which is sketched in Fig. 3. This basic loading history is divided into steps, with three symmetrical cycles repeated in each step j at a peak deformation d_j. The increase of the peak deformation per step is defined as a multiplier of the theoretical value of the yielding displacement of the specimen, d_y.

3. Experimental results: Global behaviour and failure modes

In the following the experimental results obtained in the test program are provided. In particular the cyclic behaviour and the failure modes observed for the three sets of specimens are described, and the

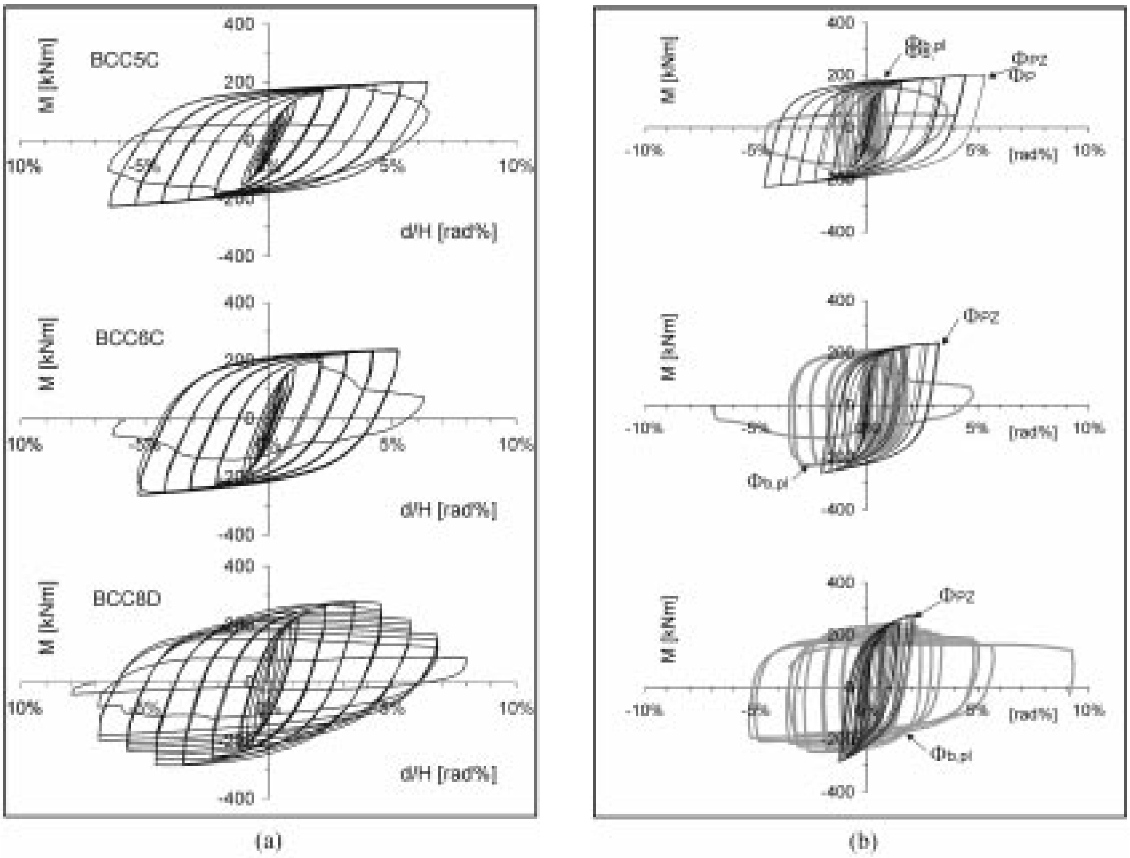

Fig. 4 (a): Moment-total rotation curves, (b): Moment-beam plastic rotation and moment-panel zone rotation curves moment rotation hysteresis loops obtained in the stepwise increasing amplitude cyclic tests are provided. In the moment rotation hysteresis loops hereafter presented, the rotation values have been calculated both as the "*unprocessed*" total rotation given by the applied interstory drift angle d/H, and as the beam rotation Φ_b, obtained through the measured LVTDs displacements at the beam cross sections. Correspondingly, in the *M-d/H* experimental curves the moment is evaluated at the centreline of the column, while in the M_b-Φ_b curves the moment is evaluated at the column face.

In Fig. 4(a) the moment-total rotation (*M-d/H*) experimental curves resulting from the BCC5C, BCC6C and BCC8D tests (cyclic increasing stepwise amplitude) are plotted, while in Fig. 4(b) both the corresponding moment - beam plastic rotation curves and the moment - panel zone rotation curves are plotted. The beam plastic rotation has been obtained through the measured displacements at the transducers 1 and 2 (see Fig. 2) by subtracting the contributions of the beam and column elastic rotations as well as of the panel zone distortion.

3.1. Specimens BCC5

As can be derived from the curves reported in Figs. 4(a) and (b), and as demonstrated also in the other tests carried out in the experimental program, the cyclic behaviour of the specimen BCC5 is characterised by a great regularity and stability of the hysteresis loops up to failure, with no deterioration of stiffness and strength properties. The very last (18^{th}) cycle presents a sudden and sharp reduction of strength, corresponding to the collapse of the specimen, which occurred due to fracture initiated in the beam flange and propagated also in the web. During the test, significant distortion of the joint panel zone has been observed, while not remarkable plastic deformation in the beam occurred.

In Table 4 a summary of the number of complete plastic cycles to collapse and the failure mode of the specimens BCC5 is reported.

Table 4 Number of plastic cycles and failure modes of BCC5 specimens

Test	No. cycles	Failure modes
A	16	Crack on the beam flange close to the weld, propagated in the beam web.
B	5	Fracture of the beam flange near the weld.
BB	4	Crack on the beam flange close to the weld, propagated in the beam web.
C	18	Crack on the beam flange close to the weld, propagated in the beam web.
D	23	Fracture of the beam flange.

Table 5 Number of plastic cycles and failure modes of BCC6 specimens

Test	No. cycles	Failure modes
A	15	Plastic hinge. Crack on the beam flange in the buckled zone, at 15 cm from the column face.
B	11	Plastic hinge. Crack on the beam flange in the buckled zone, at 10 cm from the column face.
BB	6	Plastic hinge. Crack in the beam flange close to the weld line, propagated in the beam web.
C	15	Less evident plastic hinge. Crack in the beam flange along to the weld line.
D	18	Less evident plastic hinge. Crack in the beam flange, developed close to the weld.

3.2. Specimens BCC6

Throughout the test program, two different kinds of cyclic behaviour have been observed for the BCC6 specimens. In some cases (tests C and D) the behaviour of the specimens is close to the behaviour observed for the BCC5 type, with almost no deterioration of the mechanical properties up to the last cycle, during which the collapse occurred. On the contrary, for the other tests (A, B and BB) a gradual reduction of the peak moment at increasing number of cycles is evident. In these cases, starting from the very first plastic cycles, local buckling of the beam flanges occurred, and a well defined plastic hinge has formed in the beam. In the specimens BCC6 the contribution of the panel zone deformation has not been as significant as in the BCC5 specimen type. The collapse of the specimens BCC6A and BCC6B was due to fracture of the beam flange in the buckled zone. The specimens BCC6BB, BCC6C and BCC6D failed due to fracture in the beam flange along or close to the weld line.

In Table 5 a summary of the number of complete plastic cycles to collapse and the failure mode of the specimens BCC6 is reported.

3.3. Specimens BCC8

The hysteresis loops obtained from the tests on the BCC8 specimens (except the one obtained in the C test) show a gradual reduction of the peak moment starting from the second cycle, where the maximum value of the applied moment has been usually registered. This deterioration of the flexural strength of the connection is related to occurrence and spreading of local buckling in the beam flanges and web. A well defined plastic hinge in the beam has formed in all the tested specimens. In the test C, where the specimen has been subjected to a constant amplitude rotation history, equal to 7.5% rad, an unstable behaviour of the specimen has been observed, with multiple buckling occurred in the beam flanges starting from the first plastic cycle, and a sudden failure occurred at the third plastic cycle due to the fracture in the beam flange along the weld. In the specimens BCC8 the panel zone deformation has not been remarkable, and the plastic deformation mainly took place in the beam. The collapse of the specimens BCC8A and BCC8D was due to fracture of the beam flange in the buckled zone. In the tests B, C and E the collapse of the specimens occurred due to fracture in the beam, starting along the weld or very close to the weld line.

In Table 6 a summary of the number of complete plastic cycles to collapse and the failure mode of the specimens BCC8 is reported.

Table 6 Number of plastic cycles and failure modes of BCC8 specimens

Test	No. cycles	Failure modes
A	12	Plastic hinge. Crack in the beam flange at the buckled zone, complete fracture of beam flange and web.
B	16	Plastic hinge. Crack on the beam flange along the weld line.
C	2	Multiple beam flange buckling. Crack in the beam flange close to the weld, propagated in the beam web.
D	18	Plastic hinge. Crack in the beam flange at the buckled zone.
E	15	Plastic hinge. Crack in the beam flange, developed in proximity of the weld.

4. Comparisons and observations

4.1. Panel zone and beam rotations

The contribution of the total (elastic + plastic) panel zone deformation (Φ_{PZ}) to the global rotation of the specimens (*d/H*) has been, throughout the experimental program: remarkable (in average equal to the 80% of the total imposed rotation) in the BCC5 specimens, having the smallest column section (HE160B); less significant (in average equal to the 65% of the total imposed rotation) for the BCC6 specimens, with intermediate column section (HE200B); minor (40-50% of the applied rotation) in the BCC8 specimens, characterised by the largest column section (HE240B). Consistently, the plastic rotations registered in the beam have been minor for the BCC5 specimens, comparable to the panel zone rotations in the BCC6 specimens, larger for the BCC8 specimens.

The values of the maximum total rotation (*d/H*), which, in the increasing amplitude test, reaches 0.064 rad for the BCC5 specimen, 0.053 rad for the BCC6 specimen and 0.046 rad (at a loss of strength equal to 10% of the maximum strength) for the BCC8 specimen, correspond to quite low values of beam plastic rotations ($\Phi_{b,pl}$), respectively equal to 0.0057, 0.0175 and 0.0242 rad for the three specimens, thus confirming that large rotations can be experienced thanks to column web panel deformations.

In Fig. 5 a summary of the maximum rotation values from the increasing amplitude tests is reported; in particular: the global rotation, *d/H*, the plastic rotation, $(d/H)_{pl}$, the beam plastic rotation, $\Phi_{b,pl}$, and the panel zone rotation, Φ_{PZ}, of the three specimens are provided.

4.2. Effect of the panel zone on the cyclic behaviour and failure mode

The BCC5 specimens, even though able to experience high deformation levels, have shown brittle failure modes in all the cyclic tests, with hysteresis loops practically overlaid and no degradation of the flexural strength up to the very last cycle, where a sudden decay of the carrying capacity occurred due to fracture, generally developed in the proximity of the weld. On the contrary the BCC8 specimens have exhibited a typical ductile behaviour, with formation of a well defined plastic hinge in the beam starting from the first plastic cycles, and a gradual decrease of the peak moment at increasing number of cycles up to the collapse.

These results confirm some major findings reported in (El-Tawil *et al.* 1999), where, on the basis of

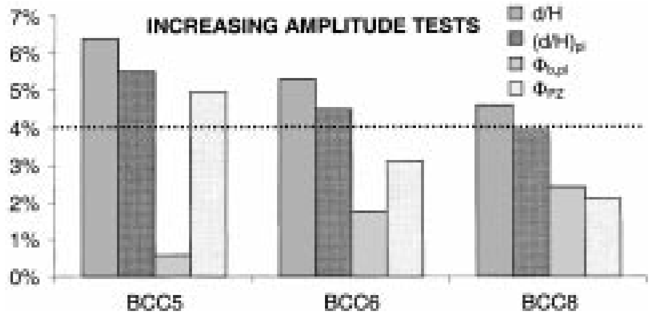

Fig. 5 Maximum rotation values from the increasing amplitude tests

FEM analyses results, it is emphasised that although weak-panel design of the beam-to-column welded connections can substantially reduce beam plastic rotation demands and effectively contribute to global connection ductility, the stress state arising at high levels of applied rotation increases the potentials for brittle fracture collapse mode of the connection. Additional results, based both on experimental tests and FEM theoretical studies are provided by (Lu *et al.* 2000), where it is found that weak column panel specimens (with PZ contributing at 70% to the total plastic rotation of the specimen) show brittle failure modes, with no previous deterioration of the strength capacity, due to fracture in the beam web weld and beam bottom flange.

The BCC6 specimens displayed a behaviour sometimes closer to the BCC5 ones (tests BCC6C and BCC6D), sometimes to the BCC8 ones (tests BCC6A, BCC6B and BCC6BB), depending on the applied loading sequence. Also with regard to the final collapse of the specimens, in the former cases it involved fracture in the beam starting at or close to the weld location, while in the latter cases it was due to the cracking in the buckled zones of the beam flanges.

4.3. Effect of the loading history on the cyclic behaviour and failure mode

Not significant effect of the loading history on the failure mode of the BCC5 specimens has been observed throughout the experimental program: all BCC5 specimens have shown a sudden collapse, corresponding to a sharp decay of the load carrying capacity of the connection and associated to a brittle fracture generally developed in the proximity of the weld.

For the BCC8 specimens the collapse occurred either due to ductile fracture in the buckled beam flange at the plastic hinge location (tests at increasing amplitude (D) and at 5% constant amplitude (A)) or due to fracture in the beam flange close to the weld location (tests at 3.75% constant amplitude, (B and E)); however in all cases a well defined plastic hinge formed in the beam and the failure of the connection occurred after that a slow degradation of the strength capacity of the specimens was observed at increasing number of cycles.

On the contrary, for the BCC6 specimens two different kinds of inelastic behaviour and collapse mode have been observed in the cyclic tests, depending on the applied loading history: for the test at increasing stepwise amplitude, C, and the test D, at the smallest constant amplitude (d/H = 3.75%), a cyclic behaviour close to the one exhibited by BCC5 specimens, with sudden decay of the strength properties of the connection and brittle fracture mode, has been observed. For the tests A, B, BB, at larger constant amplitude (d/H = 5% and 7.5%), the behaviour has been close to the one of the BCC8 specimens, with formation of a plastic hinge, slow degradation of the strength capacity and ductile fracture mode.

These observations are in line with some major findings reported by (Plumier *et a1*. 1998, Castiglioni *et al*. 2000) as result of a wide experimental program on twenty-one European type welded connections, subjected to constant cyclic amplitude loading histories. The specimens had the same beam and column cross sections, but differed in the welding details, weld access hole and presence of doubler plates. The Authors report that three different failure modes have been observed, depending on the amplitude of the cycles imposed to the specimens:

1: a failure mode B (“brittle”), under small cycle amplitude loading histories, with sudden collapse due to a crack either at the weld toes or in the base material;

2: a failure mode D (“ductile”), under large cycle amplitude loading histories, with significant and progressive deterioration of the key mechanical parameters, development of a plastic hinge and final collapse due to the gradual propagation of a crack initiating in the buckled flange zone at the

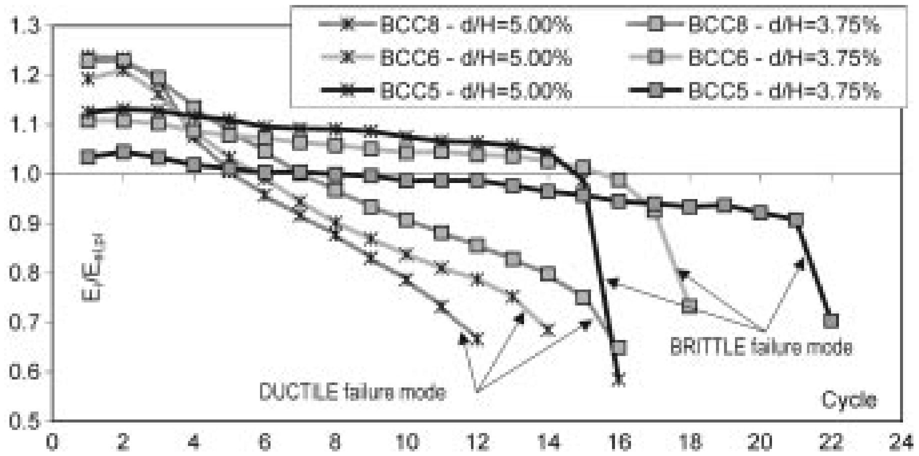

Fig. 6 Normalised cyclic energy

plastic hinge location;

3: a failure mode M (“mixed”), under cycles of intermediate amplitude, which is a combination of the two previous failure modes, since the specimen is affected by a progressive deterioration of the mechanical properties, with development of a plastic hinge and in presence of local buckling, but the collapse is due to a crack at the weld toes.

The experimental results reported in this paper suggest that for the BCC5 specimen series, independently on the applied loading history, a “brittle” failure mode occurs, due to the governing role of the panel zone in the inelastic deformation mode, which places severe demands to the beam-to-column welds. On the contrary, the dependence of the failure mode on the loading history appears evident for the BCC6 and BCC8 specimen series, when either both the beam and the panel zone (BCC6 specimens) or mainly the beam (BCC8 specimens) contribute to the inelastic deformation of the specimen.

Furthermore, in the case of “brittle” failure mode, the behaviour of the different specimens show large scatters in the fatigue endurance and in the values of cyclic performance parameters (energy, cumulated plastic rotation, etc.), while in the case of “brittle” failure mode the various specimens show a similar behaviour and close values of performance parameters in all tests. As an example in Fig. 6 the normalised cyclic energy $E_i/E_{el,pl}$ (which is the ratio between the absorbed energy in the single plastic cycle, E_i and the energy that might be absorbed in the same cycle if it had an elastic-perfectly plastic behaviour, $E_{el,pl}$) evaluated in the test at $d/H = 3.75\%$ and $d/H = 5.0\%$, is plotted against the number of cycle for the three specimens BCC5, BCC6 and BCC8. From the graph it is possible to derive the steady decrease of the normalised cyclic energy for both the BCC8 specimens, which finally experience ductile failure mode, and, on the contrary, the sudden decay, due to brittle failure mode, of the normalised cyclic energy for both the BCC5 specimens. For the BCC6 specimens, in the case of $d/H = 5.0\%$ (ductile failure mode), the first kind of trend can be derived, while in the case of $d/H = 3.75\%$ (brittle failure mode), the behaviour is close to the one observed for the BCC5 specimens.

This can be explained by considering that the plastic hinge which forms in the beam (specimens BCC8 and specimen BCC6 under $d/H = 5.0\%$) acts as a “damper”, relieving most the weld stressed;

hence, in this case, failure is achieved in the base material at the plastic hinge location and the specimen collapse is strictly related to the deterioration of the mechanical properties of the beam. On the contrary, when the specimen inelastic deformations do not occur mainly in the beam and the plastic hinge is not so evident (specimens BCC5 and specimen BCC6 under d/H = 3.75%), the welds between the beam and the column are subjected to large plastic strains, which cause sudden failures of the specimens at the weld locations.

Also the values of the cumulative plastic rotation appear highly variable for the BCC5 (values of $(d/H)_{pl,cum}$ = 0.27-0.65 rad) and BCC6 (values of $(d/H)_{pl,cum}$ = 0.30-0.73 rad) specimens, while the BCC8 specimens, excluding the test C (7.5%), show very similar values for all the tests (values of $(d/H)_{pl,cum}$= 0.48-0.55 rad).

5. Conclusions

In this paper an overview of a test program carried out on three series of welded connections has been provided, the global behaviour and the failure modes of the connections have been described, and the main differences in the performance of the three series of specimens have been emphasised. Some major aspects deriving from the analysis of the experimental data concern the effect of the loading history, of the column section and panel zone design on the cyclic behaviour, maximum rotations, energy dissipation and failure mode of the connections.

For specimens characterised by occurrence of inelastic deformations either both in the beam and in the panel zone (BCC6 specimens) or mainly in the beam (BCC8 specimens), the experimental evidence suggests a strong dependence of the cyclic behaviour, of the performance parameters values and of the failure mode on the applied loading history. On the contrary for weak panel zone specimens (BCC5 specimens) independently on the applied loading history, the same “brittle” failure mode occurs, due to the governing role of the panel zone in the inelastic deformation mode, and large scatters in the fatigue endurance and in the performance of the connections have been observed.

The quite high values of the maximum global rotations of the connections, especially if compared to the rotation capacities exhibited by US-type welded connections in past testing programs, can be related to the following aspects.

- According to the major findings reported by (Roeder & Foutch 1996, De Luca & Mele 1997), the connection rotation capacity and ductility strongly decrease as the beam depth increases. Thus higher rotations are expected for beam-to-column connections usually adopted in Europe, where the depth of the beam section (d_b = 300-450 mm) is significantly less than the ones utilised in the US practice (d_b = 500-1000 mm), due to the current adoption of perimeter frames configuration.
- Fully welded connections, as the ones adopted in the tested specimens, have already shown, in past experimental tests, higher rotation capacity than the Bolted Web Welded Flange connections (Tsai & Popov 1995, Usami *et al*. 1997), usually adopted at the US frame joints.
- A significant contribution of panel zone deformation has been observed throughout the tests, suggesting the possibility of utilising the joint panel for providing energy dissipation and stable behaviour of the connections even at large number of cycles.

However in the paper it is shown that weak panel zone connections give rise to inelastic deformation mode of the beam-column subassemblage which produces high stress concentrations at the beam to column welded zones, driving the specimen to brittle collapse mode. For this reason the contribution of panel zone distortion to the global plastic rotation of the connection should be properly calibrated in the design of the connection, through the definition of adequate values of the relative strength of beam and panel. For example, (Lu *et al*. 2000) tentatively suggest to limit the contribution of the panel zone at 50% of the total inelastic rotation. However in the authors opinion further studies on this specific topic are still needed.

References

Bertero V.V., Anderson J.C. and Krawinkler H. (1994), "Performance of steel building structures during the Northridge earthquake", Earthq. Eng. Res. Center, *Rep.UCB/EERC-94/09*, University of California, Berkeley.

Calado, L., Mele, E., and De Luca, A. (1999), "Experimental investigation on the cyclic behaviour of welded beam-to-column connections", *Proc. Eurosteel, 2nd European Conf. on Steel Structures*, PRAHA, Czech Republic, Paper No. 215.

Calado, L. and Mele, E. (2000), "Cyclic tests on bolted and welded beam-to-column connections", *ISET Journal of Earthquake Technology*, Special Issue on Experimental Techniques (in press).

Castiglioni, C.A., Bernuzzi, C. and Calado, L. "Cyclic behaviour of steel beam-to-column joints with concrete slab", *Proc. STESSA 2000, 3rd Int. Conf. on Steel Structures in Seismic Areas*, Montreal, Canada, August, A.A. Balkema, 147-154.

CEN TC250 (1992), ENV1993: Eurocode 3: Design of Steel Structures.

De Luca, A. and Mele, E. (1997), "Behaviour of steel structures in seismic zones: design aspects and research developments", *Proc. of 1st ENCMM Portugal National Meeting on Steel and Composite Construction*, Porto, Portugal, November, 589-618.

ECCS (1986), "Seismic Design. Recommended testing procedure for assessing the behaviour of structural steel elements under cyclic loads", Tech. Comm. 1 - Structural Safety and Loadings, TWG1. 3 Rep. No. 45.

El-Tawil, S., Vidarsson, E., Mikesell, T. and Kunnath, S. K. (1999), "Inelastic behaviour and design of steel panel zones", *J. Struct. Eng.* ASCE, **125**(2), 183-193.

Lu, L.W., Ricles, J.M., Mao, C. and Fisher, J.W. (2000), "Critical issues in achieving ductile behaviour of welded moment connections", *J. of Constr. Steel Res.* **55**, 325-341.

Mahin S.A., Hamburger R.O. and Malley J.O. (1996), "An integrated program to improve the performance of welded steel frame buildings", *Proc. 11th WCEE, World Conf. Earthq. Eng*., Elsevier Science Ltd., **Paper No. 1114**.

Malley J.O. (1998), "SAC Steel Project: summary of Phase-1 testing investigation results", *Eng. Structs*, **20**(4-6), 300-309.

Mele E., Calado L. and Pucinotti R. (1997), "Indagine sperimentale sul comportamento ciclico di alcuni collegamenti in acciaio", (in Italian) *Proc. 8th National Conf. Earthq. Eng. ANIDIS*, Taormina, Italy, September, 1031-1040.

Nakashima M., Suita K., Morisako K. and Maruoka Y. (1998), "Tests on welded beam-column subassemblies. I: global behaviour. II detailed behaviour", *J. Struct. Eng.* ASCE, **124**(11), 1236-1252.

Plumier A., Agatino, R., Castellani, A., Castiglioni, C.A. and Chesi, C. (1998), "Resistance of steel connections to low-cycle fatigue", *Proc.11th ECEE, European Conf. Earthq. Eng*., Paris, France, Balkema.

Roeder C.W., Foutch D.A. (1996), "Experimental results for seismic resistant steel moment frame connections", *J. Struct. Eng.* ASCE, **122**(66), 581-588.

Tanaka A., Kato, B., Kaneko, H., Sakamoto, S., Takahashi, Y. and Teraoka, M. (1997), "Seismic damage of steel beam-to-column connections evaluation from statical aspects". *Proc. STESSA 97, 2nd Int. Conf. on Steel Structures in Seismic Areas*, Kyoto, Japan, August, 856-865.

Taucer F., Negro P. and Colombo A. (1998), "Cyclic testing of the steel frame", *JRC ELSA Spec. Publ. No. I.98.160*, December.

Tsai, K.C. and Popov, E.P. (1995), "Seismic steel beam-column moment connections", In: Metallurgy, Fracture Mechanics, Welding, Moment Connections and Frame Systems Behavior. *Rep. SAC/BD-95/09*, SAC Joint Venture, Sacramento, Cal.

Usami, T., Kaneko, H., Kimura, M., Une, H. and Kushibe, A. (1997), “Real scale model tests on flange fracture behaviour of beam adjacent to beam-to-column joint and the seismic resistance after repairing and strengthening”, *Proc. STESSA 97, 2nd Int. Conf. on Steel Structures in Seismic Areas*, Kyoto, Japan, August, 955-962.

DN